Synthesis and optical characterization of Pd–Au bimetallic nanoparticles dispersed within monolithic mesoporous silica

Cuncheng Li, Weiping Cai *, Caixia Kan, Ganhua Fu

Institute of Solid State Physics, Chinese Academy of Sciences, Nano-materials Laboratory, Science Island, Hefei 230031, Anhui, PR China

Abstract

Au–Pd bimetallic nanoparticles dispersed within pores of monolithic silica was synthesized by soaking Au nanoparticles contained silica host into Pd precursor solution and subsequent step-annealing at temperature from 373 to 773 K. Theoretical optical spectra based on Mie-like model for $Au_{core}Pd_{shell}$ nanoparticles yield excellent agreement with the experimental results.
© 2004 Acta Materialia Inc. Published by Elsevier Ltd. All rights reserved.

1. Introduction

Bimetallic nanoparticles, in which two kinds of metals are contained in one particle, have been attracted great interest, for their unique catalytic, electronic, and optical properties compared with those of corresponding monometallic nanoparticles [1–5]. One of the most popular examples is gold–palladium (Au–Pd) system, which is miscible at any ratio, due to unique catalytic and optical properties, especially for $Au_{core}Pd_{shell}$ nanoparticles [2–4]. There are many methods reported on their preparation in solution, including alcohol reduction [2,4], sonochemical method [3], citrate reduction [6,7] etc. In the last decade, extensive studies have been focused on non-supported bimetallic nanoparticle dispersions. From the practical point of view, however, it is more important to disperse and stabilize these functional nanoparticles in a bulk solid material. To our knowledge, there has been no study about bimetallic nanoparticles dispersed in a bulk solid so far, although bimetallic nanoparticles immobilized on surface of oxide powders have been reported [8–10], Recently, we have synthesized Au/Pd bimetallic nanoparticles, with core/shell and alloying structure, confined within monolithic mesoporous silica, by soaking Au nanoparticle-contained silica into Pd precursor solution and subsequent step-annealing, and found that this material exhibits strong environment sensitivity and unique optical properties, which will be reported elsewhere. Here we focus on the synthesis and the optical characterization of Au/Pd bimetallic nanoparticles dispersed within monolithic mesoporous silica.

2. Experimental

Monolithic porous silica host (planar-like, 0.5 mm in thickness) was prepared from the tetraethylorthosilicate, alcohol, distilled water by the sol–gel technique, drying and finally annealing in air at 973 K for 1 h in air, as previously described [11]. The pores in the preformed host are interconnected and open to ambient, its specific surface area and porosity ware estimated to be about 540 $m^2 g^{-1}$ and 45%, respectively, and pore diameters are mainly distributed in the range smaller than 20 nm, determined by isothermal N_2 adsorption measurement as previously described [12]. The monolithic porous silica was immersed into chloroauric acid ($HAuCl_4 \cdot 4H_2O$) solution at room temperature (298 K), and the concentrations of chloroauric acid were 10, 15, 20, 30 mM (milli mole/liter), respectively. After a sufficient soaking time (about two weeks), the sample was taken out and washed with deionized water, then annealed in N_2–H_2 (N_2:H_2 = 1:1) mixed gas at 773 K for 2 h, to reduce gold

* Corresponding author. Tel.: +86-5515592747; fax: +86-5515591434.

E-mail address: wpcai@issp.ac.cn (W. Cai).

ions and form gold nanoparticles within the pores of silica, thus forming the Au/silica composite. The Pd/silica composite was prepared by the same method but using $PdCl_2$ solution.

Afterward, the Au/silica samples were immersed into $PdCl_2$ solution at room temperature for two weeks before they were taken out and washed with deionized water. The samples were then step-annealed in the N_2–H_2 mixed gas starting from 373 to 773 K with step of 100 K for 1 h, respectively. The total concentration of $HAuCl_4$ and $PdCl_2$ was kept to be 30 mM. We obtained Au–Pd/silica-X (X represents the annealing temperature before measurement) composite with the ratios of Pd to Au (1:2, 1:1, 2:1) by changing the concentration of $HAuCl_4$ and $PdCl_2$ solution. The molar ratio of (Au + Pd) to SiO_2 can be estimated to be about 0.07:100 by the total concentration of the solution (30 mM) and the host porosity (45%), as previously reported [11].

Isothermal nitrogen sorption measurement was conducted using an Omnisorp 100CX specific surface area and porosity analyzer. For transmission electron microscopic (TEM) observation, the samples were ground into powders and dispersed in alcohol in a test tube, followed by ultrasonic vibration in a bath for 10 min. A few drops of the liquid were placed on a carbon coated copper grid. After evaporation of the alcohol, the copper grid was mounted on a JEOL 2010 transmission electron microscope, operating at an accelerating voltage of 200 kV. Optical absorption spectra for all samples were recorded with a CARY 5E UV–VIS–NIR dual-beam spectrophotometer in the 200–1500 nm wavelength range.

3. Results

It has been shown that the measured specific surface area decreases significantly from 540 $m^2 g^{-1}$ for the reference sample silica host to 523 $m^2 g^{-1}$ for the Au/silica and 498 $m^2 g^{-1}$ for Pd–Au/silica-573 (Pd:Au = 1:1). This decrease can be attributed to the presence of particles within the pores of the silica. These particles within pores make it difficult for nitrogen molecules to enter the too small free space during nitrogen sorption measurement; hence, the partial area of the pores could not be measured, as previously described [12]. The presence of particles within pores is more clearly shown by the nitrogen sorption isotherms of the corresponding undoped and doped samples, as shown in Fig. 1, in which the curve for host is higher than those for doped samples in the whole pressure region.

Because the metal nanoparticles were recessed inside the mesopores of silica, it is very difficult to identify them directly in TEM fields except amorphous silica aggregates, as typically illustrated in Fig. 2 (for the Pd–Au/silica-573 (Pd:Au = 1:1) sample). The correspond-
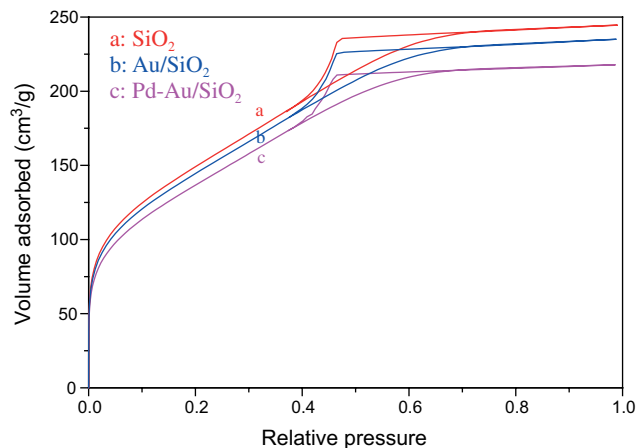

Fig. 1. Nitrogen sorption isotherms of: (a) silica host, (b) 15Au/SiO$_2$ sample (prepared by immersing the host into 15 mM HAuCl$_4$ solution, then annealing at 773 K in H$_2$–N$_2$ (H$_2$:N$_2$ = 1:1) mixed gas for 2 h) and (c) Pd–Au/SiO$_2$-573 (Pd:Au = 1:1) sample prepared by step-annealing from 373 to 573 K in H$_2$–N$_2$ (H$_2$:N$_2$ = 1:1) mixed gas.
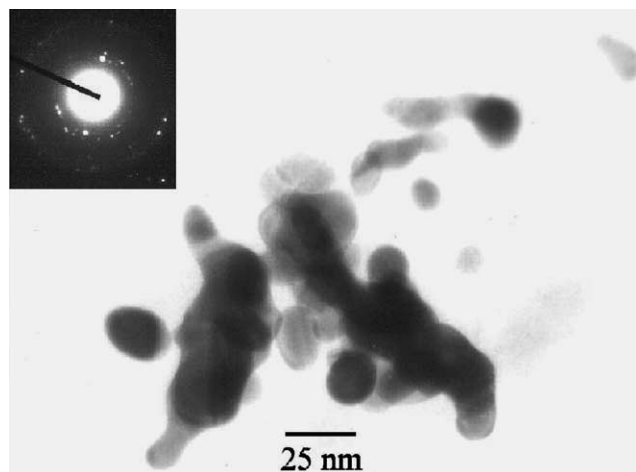

Fig. 2. TEM photograph for Pd–Au/SiO$_2$-573 (Pd:Au = 1:1).

ing selected area electron diffraction, however, confirmed existence of the metal particles with face-centered cubic structure, a shown in inset of Fig. 2. The calculations of crystal plane spacings from the diffracted rings are in agreement with data of both Au and Pd, but we cannot distinguish Au or Pd due to identical structure and similar lattice constants (<4.6% in difference). Here we try to characterize it from optical measurements as follows.

The optical absorption spectra for Pd–Au/SiO$_2$-X (Pd:Au = 1:1) and Au/silica (15 mM) sample are shown in Fig. 3. For the latter, there is an absorption band peaking around 545 nm, which is the well-known surface plasmon resonance (SPR) of Au nanoparticles [13]. The peaks around 1370 and 1400 nm are from silica, and will not be discussed here. Compared with the sample Au/silica (15 mM), the Au SPR in Pd–Au/SiO$_2$-373
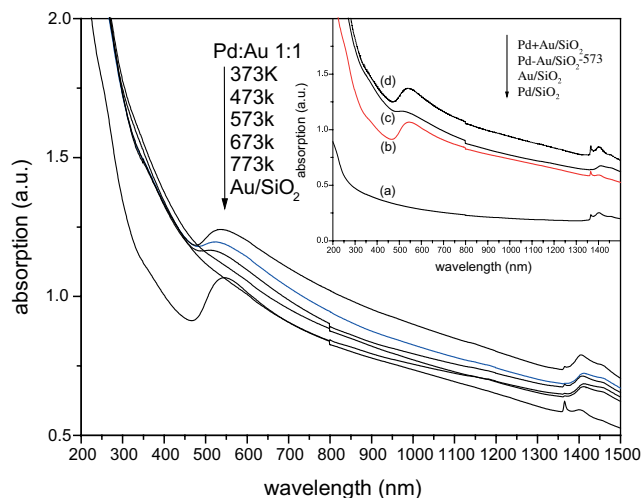
Fig. 3. The optical absorption spectra for Pd–Au/SiO$_2$-X (Pd:Au = 1:1) and Au/silica (15 mM) samples, inset: optical absorption spectra for (a) Pd/SiO$_2$ (15 mM), (b) Au/SiO$_2$ (15 mM), (c) Pd–Au/SiO$_2$-573 (Pd:Au = 1:1), (d) superimposing of (a) and (b).

sample blue-shifts (about 10 nm) and damps, but the background of the optical absorption spectrum increases obviously due to additional existence of Pd nanoparticles. The Au SPR decreases and blue-shifts, accompanied by decrease of background, with increasing annealing temperature up to 673 K, at which the SPR almost vanishes. It is evident that the spectra for Pd–Au/SiO$_2$ are obviously different from superimposing spectrum of Pd/SiO$_2$ (15 mM) and Au/SiO$_2$ (15 mM) or that of physical mixture of Pd and Au nanoparticles in silica, see the inset of Fig. 3.

For the samples Pd–Au/SiO$_2$-X with different ratios of Pd to Au, the optical spectra exhibit similar results to those with the ratio Pd:Au = 1:1, as shown in Fig. 4, while the annealing temperature, at which the SPR disappears, decreases with increase of the ratio of Pd to Au in sample.
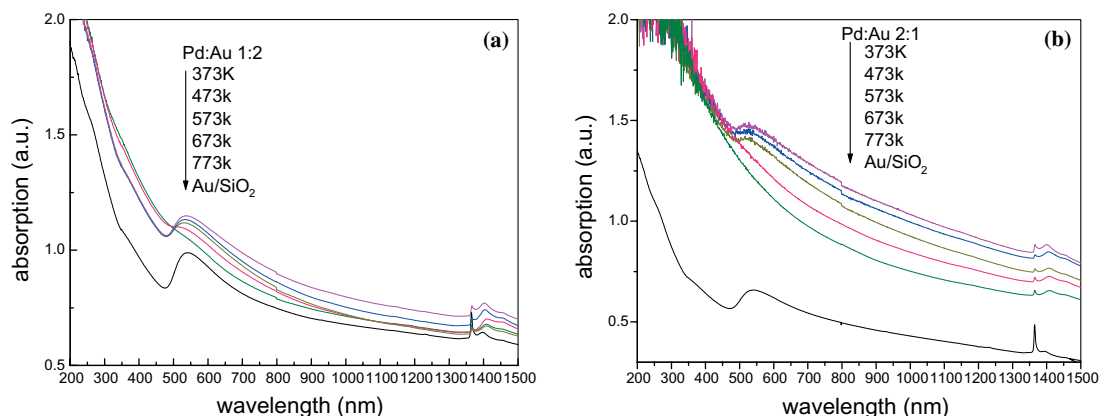
4. Discussions

4.1. Formation of core/shell structure

Unlike Au nanoparticles, whose SPR is in the visible region, the maximum absorption of Pd nanoparticles is located at about 220 nm [14]. For Pd–Au/SiO$_2$-373 composites, an increase of the background, in comparison with that of Au/SiO$_2$ samples, originates from additional existence of pure Pd nanoparticles in silica. Comparing the optical absorption spectra of the Pd–Au/silica-X with superimposing spectra of separately prepared monometallic nanoparticles in silica, we can conclude that the colloidal dispersions in the Pd–Au/silica-X sample are basically not composed of simple mixture of pure Au and Pd nanoparticles.

The blue-shift and damp of the Au SPR, for the sample Pd–Au/silica-373, can be attributed to formation of the Au$_{core}$Pd$_{shell}$ nanoparticles in silica. After the sample Au/SiO$_2$ was soaked in PdCl$_2$ solution and subsequently dried, within the pores of silica, in addition to existence of some pure PdCl$_2$ nanoparticles, the pre-formed Au nanoparticles would be wrapped with PdCl$_2$ shell. In the following treatment at 373 K in reductive atmosphere, the PdCl$_2$ nanoparticles will form Pd nanoparticles, whereas the Au nanoparticles wrapped with PdCl$_2$ shell form the Au$_{core}$Pd$_{shell}$ nanoparticles.

It is well-known that the electron density in surface layer of metals nanoparticles can greatly influence their SPR position and an increase of the electron density will cause a blue-shift of the SPR [13,15,16]. On the other hand, the surface electron density of metal particles can be greatly affected by changing their chemical surroundings, such as chemical adsorbate on the particle surface [17]. Therefore, the observed blue-shift of Au SPR can be attributed to an increase of the surface electron density of Au nanoparticles at the expense of the electrons from the adsorbate of the post-reduced Pd

Fig. 4. The optical absorption spectra of Pd–Au/SiO$_2$-X sample with the ratios of Pd/Au are (a) 1:2 and (b) 2:1, respectively.

atoms due to their different electron concentrations (Pd: 13.4×10^{22} cm^{-3}, Au: 5.9×10^{22} cm^{-3}).

The damping and even disappearance of the Au SPR for the Pd–Au/silica-X are consistent with the previous observations that the presence of a group 10 metal ($d^8 s^2$) in bimetallic nanoparticles suppresses the surface plasmon energies of group 11 metal ($d^{10} s^1$) [18–20], and imply the formation of Au–Pd bimetallic nanoparticles in our samples. Taking into consideration of the sequential synthesis in our experiments, it is reasonable to suggest that when the annealing temperature is low or for Pd–Au/silica-373, the formed Au–Pd bimetallic nanoparticles are Au core/Pd shell structured.

It is evident that Au$_{core}$Pd$_{shell}$ particles should be larger than the pure Pd particles for the most ones. As reported elsewhere [12], some larger particles within pores of silica are found to grow upon annealing, while the others became smaller and smaller, comparable to Ostwald ripening [21] where larger particles grow at the expense of smaller ones. Consequently, with increase of step-annealing temperature, the thickness of Pd shell on Au nanoparticles would increase through diffusion of Pd atoms from the smaller Pd particles existing in silica to the surface of Au$_{core}$Pd$_{shell}$ particles along the pore wall or channels. The rise of the shell would result in continuous blue-shift and decrease of the SPR. Here we should mention, however, that during formation and thickness increase of the shell, the alloying on the interface between Au core and Pd shell should also occur. Obviously, when annealing temperature is low enough, say, 373K, the increase of shell layer should dominate, whereas annealing at enough high temperature, alloying would be dominative.

4.2. Mie-like model

In order to quantitatively analyze the above results, theoretical calculation was conducted. Based on the existence of local porosity at the interface of particle/matrix, we can equivalently describe a particle within the pore of host by a multi-layer core/shell model, as schematically shown in Fig. 5. The local porosity is simplified to be a hollow shell surrounding the core/shell structured particle with a thickness d_m which is a measurement of the porosity. This is a two-shell problem. The dielectric data for Au and Pd are from the references [22] and [23], respectively, which were modified by size-dependent electron scattering (see Eq. (8) in Ref. [24]). Based on the Mie-like model [25,26], which can well-describe the optical absorption property of bimetallic nanoparticles in dielectric matrix, according to recurrence solution, as previously in detail described [26], we can obtain the theoretical extinction spectra of Au$_{core}$Pd$_{shell}$ nanoparticles, letting the dielectric constant of silica 2.25, $d_m = 0.25$ nm for the 45% of porosity as previously reported [27]. Fig. 6 illustrates a series of calculated results of Au$_{core}$Pd$_{shell}$ nanoparticles with different thickness of Pd shell. It can be seen that the formation of Pd shell on Au surface strongly suppresses the Au SPR and results in its blue-shift. Continual increasing of the shell thickness induces ever blue-shifting and leads to disappearance of the Au SPR, which is in good agreement with our results, shown in Figs. 3 and 4.

Further, taking into account of possible alloying at the core/shell interface during step-annealing, here we assume that the dielectric function of an alloyed shell takes the form [28]: $\varepsilon(x) = (1 - x)\varepsilon_{Pd} + x\varepsilon_{Au}$ where x is the mole fraction of Au and ε is the dielectric constant.

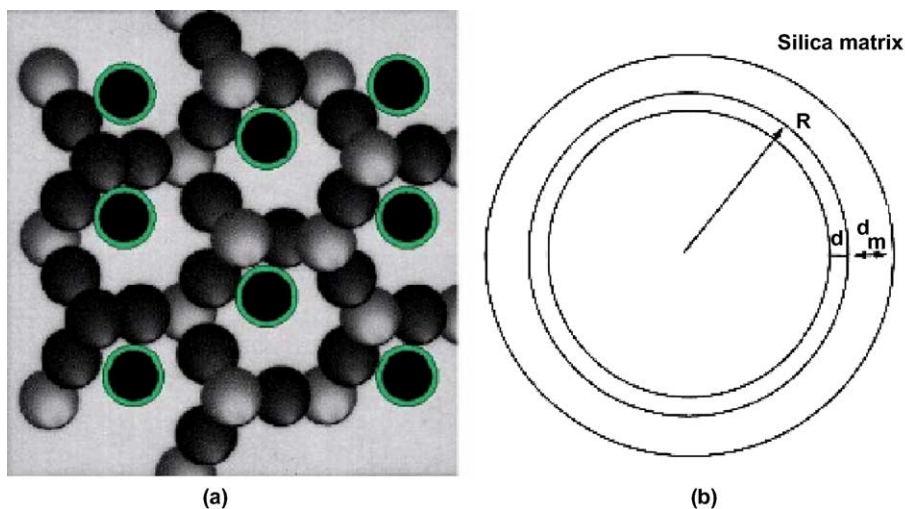**Silica matrix**

(a)   (b)

Fig. 5. Schematic drawing of: (a) core/shell structured nanoparticle within the pores of monolithic silica (network represents silica skeleton) and (b) the multi-layer core/shell model for a core/shell particle (see text). R: the radius of the particle, d: thickness of metal shell; d_m: thickness of the hollow shell.
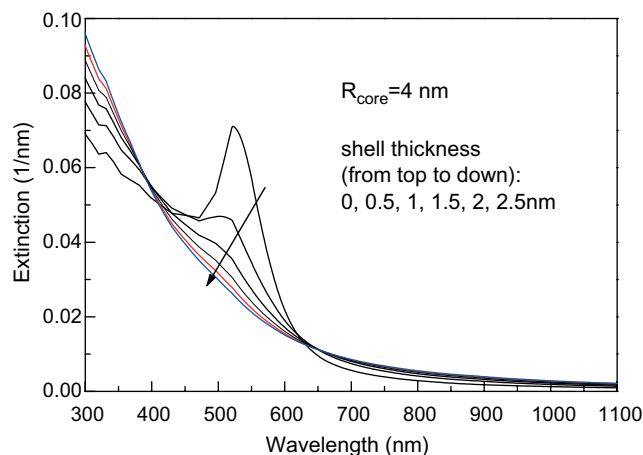
Fig. 6. Calculated extinction spectra of $Au_{core} Pd_{shell}$ nanoparticles with different thickness of Pd shell (the radius of Au core is: 4 nm).

With the same method as above, we can thus obtain the theoretical extinction spectra of Au core/Au–Pd alloying shell particles in silica. Fig. 7 illustrates the results for a given sized core/shell structured particle with different thickness of alloyed shell (where *x* is 0.5). We can see, like pure Pd shell, that the formation of Au–Pd alloyed shell also suppresses the Au SPR and induces its blue-shifting, but can not result in disappearance of the Au SPR. In other words, in the temperature range studied here, the decrease and disappearance of Au SPR with rise in step-annealing temperature (see Figs. 3 and 4) can mainly be attributed to the increase of Pd shell. Obviously, for a sample with higher ratio of Pd to Au, the thickness of Pd shell increases faster with increase of the step-annealing temperature, and the temperature, at which the Au SPR vanishes, is lower (see Figs. 3 and 4). However, some questions remain, such as, the growth

mechanism of shell layer, orientation relation between core and shell crystals, alloying extent at the interface and its temperature dependence, which are now in progress.

5. Conclusions

We have, for the first time, reported assembly of $Au_{core}Pd_{shell}$ nanoparticles into monolithic mesoporous silica by soaking and subsequent step-annealing, and presented optical characterization of its structure. The formation of Pd shell on Au particles results in decrease and blue-shifting of the Au SPR. With increase of step-annealing temperature, the Au SPR ever-decreases and even disappears mainly due to ever-increasing of Pd shell layer through diffusion of Pd atoms from the smaller Pd particles existing in silica to the surface of $Au_{core}Pd_{shell}$ particles along the pore wall or channels. It means that we can control the optical properties of this assembly by changing the shell thickness. In our experimental temperature range, the increase of Pd shell layer dominates, whereas alloying at the interface of core/shell is relatively not obvious during step-annealing.

Acknowledgements

References

[1] Chen YH, Nickel U. J Chem Soc, Faraday Trans 1993;89:2479.
[2] Toshima N, Harada M, Yamazaki Y, Asakura K. J Phys Chem 1992;96:9927.
[3] Lee AF, Baddeley CJ, Hardacre C, Ormerod RM, Lambert RM. J Phys Chem 1995;99:6096.
[4] Harada M, Asakura K, Toshima N. J Phys Chem 1993;97:5103.
[5] Michaelis M, Henglein A, Mulvaney P. J Phys Chem 1994;98:6212.
[6] Mizukoshi Y, Fujimoto T, Nagata Y, Oshima R, Maeda Y. J Phys Chem B 2000;104:6028.
[7] Mizukoshi Y, Okitsu K, Maeda Y, Zamamoto TA, Oshima R, Nagata Y. J Phys Chem B 1997;101:7033.
[8] Okitsu K, Murakami M, Tanabe S, Matsumoto H. Chem Lett 2000:1336.
[9] Lam YL, Boudart M. J Catal 1977;50:530.
[10] Giorgio S, Chapon C, Henry CR. Langmuir 1997;13:2279.
[11] Cai W, Zhang L. J Phys: Condens Matter 1997;9:7257.
[12] Cai W, Zhang L, Zhong H, He G. J Mater Res 1998;13:2888.
[13] Kriebig U, Vollmer M. Optical properties of metal clusters. Berlin: Springer; 1995.
[14] Henglein A. J Phys Chem B 2000;104:6683.
[15] Mulvaney P, Giersig M, Henglein A. J Phys Chem 1992;96:10419.
[16] Cai W, Hofmeister H, Dubiel M. Eur Phys J D 2001;13:245, 2001;14:397.
[17] Henglein A, Mulvaney P, Holzwarth A, Sosebee TE. Ber Bunsenges Phys Chem 1992;96:754.
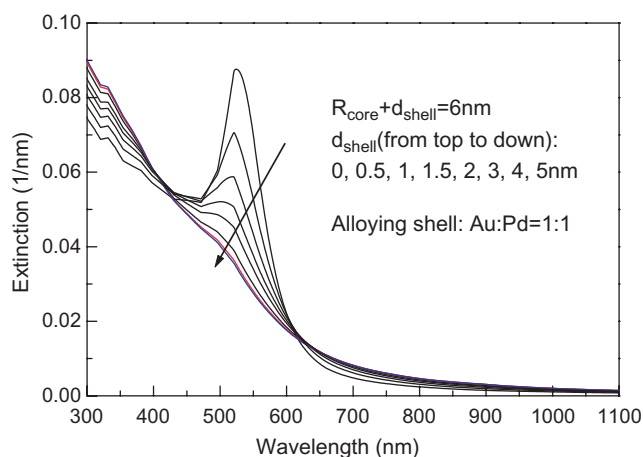

Fig. 7. Calculated extinction spectra for a given sized Au core/alloyed shell nanoparticle (6 nm in radius) with different thickness of shell (in shell layer, Au:Pd = 1:1).

[18] Toshima N, Yonezawa T. New J Chem 1998;22:1179.

[19] Liu H, Mao G, Meng S. J Mol Catal 1992;74:275.

[20] Mizukoshi Y, Okitsu K, Maeda Y, Yamamoto TA, Oshima R, Nagata Y. J Phys Chem B 1997;101:7033.

[21] Verhoeven JD. Fundamentals of physical metallurgy. New York: John Wiley; 1975.

[22] Johnson PB, Christy RW. Phys Rev B 1972;6:4370.

[23] Johnson PB, Christy RW. Phys Rev B 1974;9:45056.

[24] Hoevel H, Fritz S, Hilger A, Kreibig U, Vollmer M. Phys Rev B 1993;48:18178.

[25] Sinzig J, Quinten M. Appl Phys A 1994;58:157.

[26] Cai W, Hofmeister H, Rainer T, Chen W. J Nanoparticles Res 2001;3:443.

[27] Lerme J, Palpant B, Prevel B, Pellarin M, Treilleux M, Vialle JL, et al. Phys Rev Lett 1998;80:5105.

[28] Mulvaney P. Langmuir 1996;12:788.